An automated distinction of DICOM image for lung cancer CAD system

H. Suzuki*[a], S. Saita[b], M. Kubo[b], Y. Kawata[b], N. Niki[b], H. Nishitani[c]
H. Ohmatsu[d], K. Eguchi[e], M. Kaneko[f], and N. Moriyama[g]

[a] Systems Innovation Engineering, Graduate School of Advanced Technology and Science, The University of Tokushima, 2-1 Minami-Josanjima-cho, Tokushima, 770-8506 Japan
[b] Institute of Technology and Science, The University of Tokushima Graduate School,
[c] Institute of Health Biosciences, The University of Tokushima Graduate School
[d] National Cancer Center Hospital East
[e] Teikyo University, School of Medicine
[e] National Cancer Center Hospital
[e] National Cancer Research Center for Cancer Prevention and Screening

Abstract

Automated distinction of medical images is an important preprocessing in Computer-Aided Diagnosis (CAD) systems. The CAD systems have been developed using medical image sets with specific scan conditions and body parts. However, varied examinations are performed in medical sites. The specification of the examination is contained into DICOM textual meta information. Most DICOM textual meta information can be considered reliable, however the body part information cannot always be considered reliable. In this paper, we describe an automated distinction of DICOM images as a preprocessing for lung cancer CAD system. Our approach uses DICOM textual meta information and low cost image processing. Firstly, the textual meta information such as scan conditions of DICOM image is distinguished. Secondly, the DICOM image is set to distinguish the body parts which are identified by image processing. The identification of body parts is based on anatomical structure which is represented by features of three regions, body tissue, bone, and air. The method is effective to the practical use of lung cancer CAD system in medical sites.

Keywords: DICOM, CAD, Examined body part, X-ray CT

1. INTRODUCTION

Lung cancer screening consists of frontal and lateral chest X-rays and sputum cytology. However, there are anatomical blind spots on chest X-rays. Detecting the cancer on the spot is difficult. Recently, helical (spiral) CT was developed. There are no anatomical blind spots on CT image. Therefore, lung cancer screening has been performed using CT [1]-[3]. In the lung cancer CT screening, CT generates many more images than x-ray. The problem is how to reduce the work of radiologists. To solve the problem, Computer-aided Diagnosis (CAD) has been expected [4], [5].

In the medical sites which lung cancer CT screening have been conducted, the images vary in the modality and the scan conditions. The image variation affects the quantitative analysis of CAD [6]. Therefore, the automated method of image distinction for CAD is necessary.

The scan conditions are written in DICOM header information [7]. Some of the textual meta information is generated by the modality at the examination. For example, there are X-ray tube current and voltage. Most DICOM textual meta information can be considered reliable. However, the examined body parts may be not written [8].

Lehman suggested a method [9]. This method uses content-based image retrieval (CBIR). In the method, incorrect identification occurs with insufficient data. It is necessary to construct the databases by various scan conditions.

We have developed an examined body part identification which implements two requirements. Firstly, the method can support variation in the scan conditions. Secondly, the method can identify five body parts, head, neck, chest, abdomen, and pelvis from whole body.

Medical Imaging 2009: Advanced PACS-based Imaging Informatics and Therapeutic Applications
edited by Khan M. Siddiqui, Brent J. Liu, Proceedings of SPIE Vol. 7264, 72640Z · © 2009 SPIE
CCC code: 1605-7422/09/$18 · doi: 10.1117/12.811396

Section 2 describes the overview of the automated distinction of DICOM images, and of the distinction by DICOM textual meta information. Section 3 describes the examined body part identification.

2. AUTOMATED DISTINCTION OF DICOM IMAGE

2.1 DICOM image

The scan conditions of image are written in the DICOM textual meta information. Table.1 shows scan conditions of a CT image. The image was acquired by lung cancer CT screening. It is possible to distinguish lung cancer CT images by the DICOM textual meta information, where scan conditions are usually written. We surveyed the scan conditions of DICOM textual meta information at 8 medical sites. Table.2 shows the result. The 11 scan conditions had been written at all 8 medical sites, but only at 3 medical sites, the examined body part had been written.

2.2 Automated distinction of DICOM image

The body part information cannot always be considered reliable. However, the other 11 scan conditions can be considered reliable. Our method consists of two steps. In first step, CT images are distinguished by the textual meta information. In the second step, the examined body parts of CT images are identified using image data. Figure.1 shows the procedure of automated distinction of DICOM image.

Table.1. Image scan condition of lung cancer CT screening.

Modality	CT
Image type	Axial
Contrast	none
Patient position	Supine position
Image size [pixel]	512×512
Pixel size [mm]	0.625×0.625
X-ray tube voltage [kV]	120
X-ray tube current [mA]	50
Slice thickness [mm]	10
Reconstruction interval [mm]	10
Convolution kernel	FC01
Examined body part	Chest

Table.2. Survey result of scan conditions in DICOM textual meta information at 8 medical sites.
Model A is TOSHIBA Aquilion, Model B is SIEMENS Sensation, and Model C is GE LightSpeed.
O means the element was written, and X means the element was not written.

	Site A	Site B	Site C	Site D		Site E	Site F	Site G	Site H
	Model A	Model A	Model A	Model A	Model B	Model C	Model A	Model A	Model A
Modality	O	O	O	O	O	O	O	O	O
Image type	O	O	O	O	O	O	O	O	O
Contrast	O	O	O	O	O	O	O	O	O
Patient position	O	O	O	O	O	O	O	O	O
Image size	O	O	O	O	O	O	O	O	O
Pixel size	O	O	O	O	O	O	O	O	O
X-ray tube voltage	O	O	O	O	O	O	O	O	O
X-ray tube current	O	O	O	O	O	O	O	O	O
Slice thickness	O	O	O	O	O	O	O	O	O
Reconstruction interval	O	O	O	O	O	O	O	O	O
Convolution kernel	O	O	O	O	O	O	O	O	O
Examined body part	X	X	X	O	O	X	O	X	O

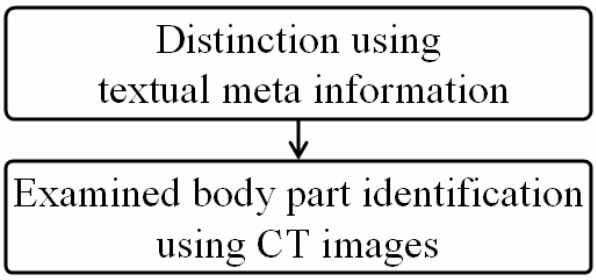

Fig.1. Procedure of automated distinction of DICOM image

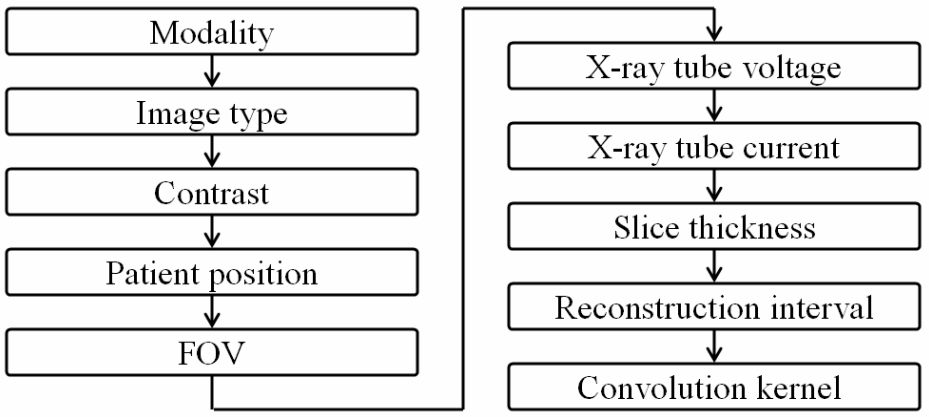

Fig.2. Procedure of distinction using textual meta information.

2.3 Distinction using textual meta information

Figure.2 shows the procedure of distinction using textual meta information. The FOV is used for distinction of CT images which were acquired from chest, abdomen, or pelvis examination. The threshold of FOV is determined by the following survey result. We surveyed the size of FOV using various CT images. The survey used 3 kind of CT images, (a) CT images of chest, abdomen, and pelvis, (b) CT images of head, neck, and upper extremity, (c) High resolution CT images of skull, lung, and spine. Figure.3 shows the survey result. A plot means CT image set of an examination. The result indicates size of FOV is effective for distinction of CT images which were acquired from chest, abdomen, or pelvis examination.

3. EXAMINED BODY PART IDENTIFICATION USING CT IMAGES

The body parts vary in the anatomical structure. In particular, the features of skeleton are important for identification of the body parts, because the bone is distributed throughout the body. The distinctive feature of chest is air, because the lung has wide air space. For convenience, the difference between bone, air and body tissue on CT image is taken as big difference.

Based on the above focus, our method consists of 5 steps as shown in Figure.4, (1) segmentation of bone, body tissue, and air, (2) description of bone, body tissue, and air, (3) multilayer structure extraction, (4) Structure element extraction, (5) Examined body part identification based on rules.

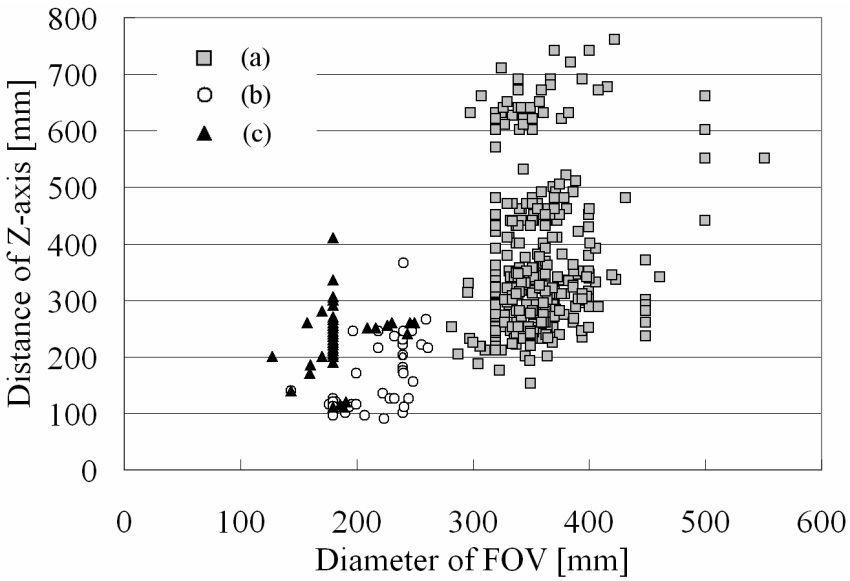

Figure.3. Survey result of FOV size. (a) CT images of chest, abdomen, and pelvis, (b) CT images of head, neck, and upper extremity, (c) High resolution CT image of skull, lung, and spine.

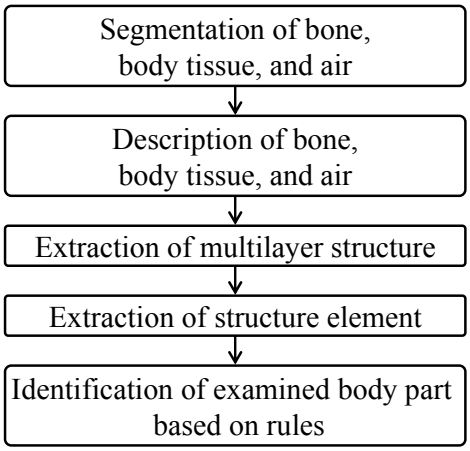

Figure.4. Procedure of examined body part identification.

3.1 Segmentation of bone, body tissue, and air

The regions of bone, body tissue, and air are segmented from CT image. The three regions are segmented by threshold of CT value. The CT value of bone is high, and the CT value of air is low. The CT value of body tissue is between the bone and air. The result is shown in Figure.5 (a).

3.2 Description of bone, body tissue, and air

The segmented bone, body tissue, and air are roughly described. The converted image is computed using Slab MIP, closing, and reduction of small regions. Using the Slab MIP, label image set of step.1 is converted to set of part image set. The steps following this step are applied to each part image set. The closing is a dilation followed by an erosion operation. The filter shape is set to a circle. The result is shown in Figure.5 (b).

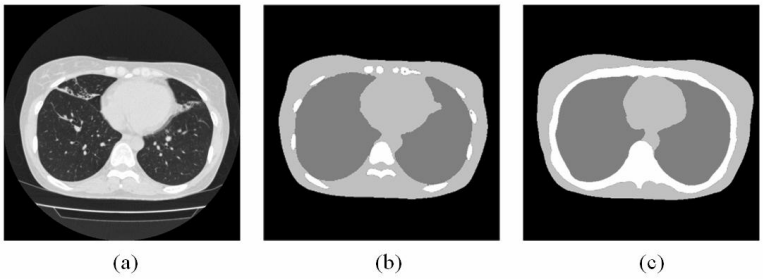

Figure.5. Description result of bone, body tissue, and air. (a) Original image, (b) Segmentation result of bone, body tissue, and air, (c) Description result of bone, body tissue, and air.

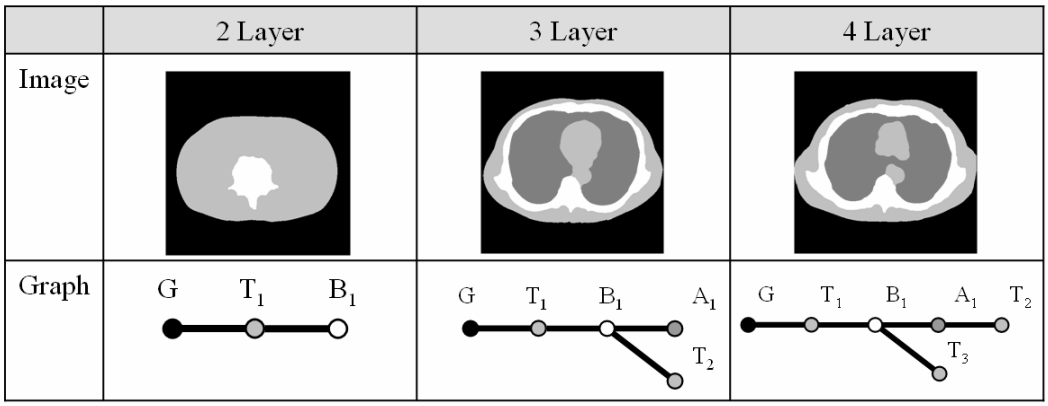

Figure.6. Examples of multilayer structure.

3.3 Extraction of multilayer structure

We focused on the multilayer structure of the bone, body tissue, and air, because the anatomical structure has relationship with other included parts. For instances, the skin includes the muscle and fat, and they includes organ and bone. The multilayer structure consists of upper layer and lower layer. In the labeled image by step.2, the regions which have holes are upper layer, and the regions of holes are lower layer. The multilayer structure is expressed using graph. Figure.6 shows examples of the graph. The node G is a region of background, the node B is a region of bone, the node T is a region of body tissue, and the node of A is a region of air. The nodes and edges have attributes. The attributes of the node are rectangle area, rectangle aspect ratio of the regions. The attributes of connections is vector between the upper layer and lower layer. The attributes are normalized.

The normalized rectangle area of the node S_{NL} is computed using Eq. (1). The S_L and S_U represent the rectangle area of normalized node and the rectangle area of upper layer node of it.

$$S_{NL} = S_L / S_U \tag{1}$$

The normalized vector length V_{NS} is computed using Eq. (2). The V_S and K_U represent the vector length of normalized edge and rectangle diagonal length of upper layer node in the edge.

$$V_{NS} = \frac{V_S}{K_U \times 0.5} \tag{2}$$

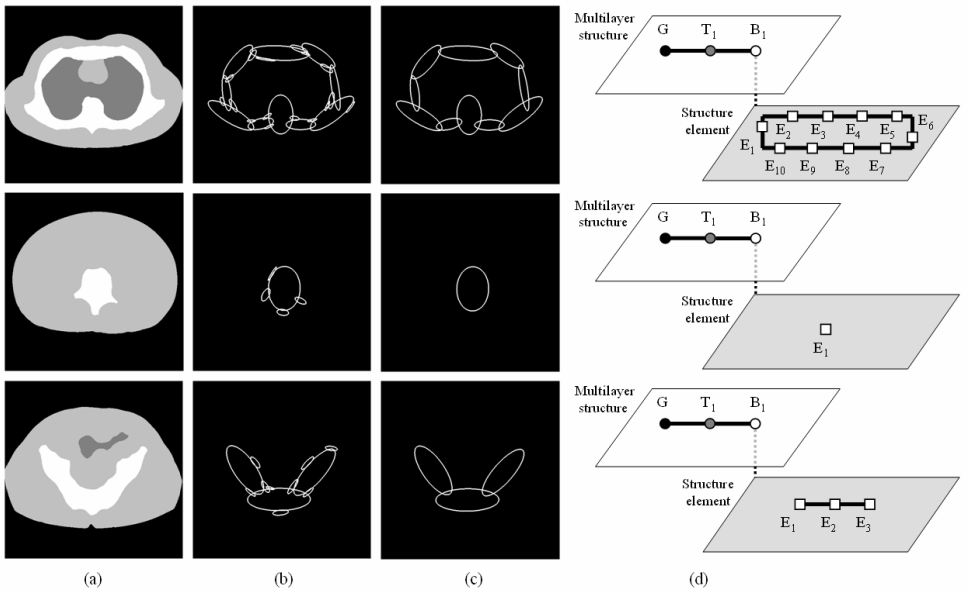

Figure.7. Results of structure element extraction. (a) Description of bone, body tissue, and air, (b) Result of Ellipsoid-Expansion, (c) Select of major structural ellipsoid, (d) Graph of multilayer structure and structure element.

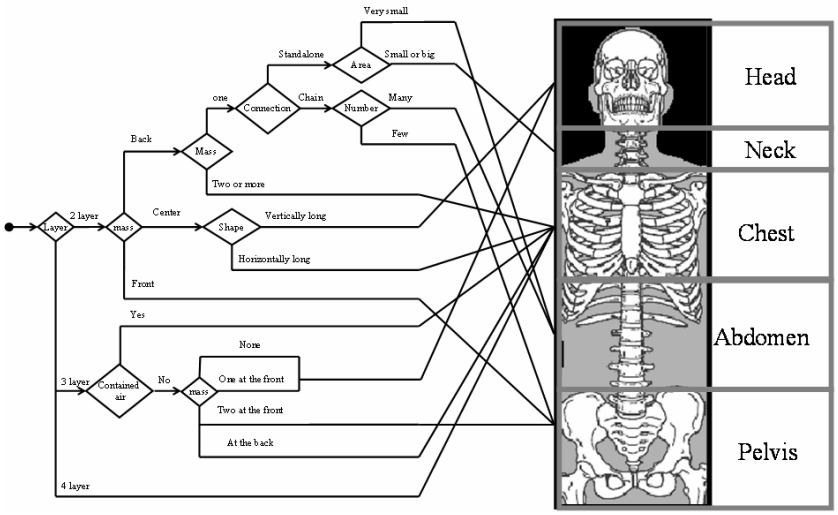

Figure.8. Rules of examined body part identification.

3.4 Extraction of structure element

The layer consists of structure elements. We show the structure element using ellipsoid. In the past study, the description of a binary image using Ellipsoid-Expansion was suggested [10]. The Ellipsoid-Expansion method is not influenced by details of the shape of the object and withstands shifts, change of scaling, and rotation of the shape. In this step, the bone, body, and air regions are expressed using the Ellipsoid-Expansion. In result of the method, some ellipsoids are not major. Therefore, major ellipsoids are selected. The selection keeps structure. The result is shown in Figure.7.

Tble.3. Scan conditions of CT image sets for experiment.

	Torso CT image set	Chest CT image set	Chest CT image set
Model name	Aquilion	Aquilion	Aquilion
Contrast	None	None	None
Image size [pixel]	512x512	512x512	512x512
Pixel size [mm]	0.582 - 0.976	0.625	0.625
X-ray tube voltage [kV]	120	120	120
X-ray tube current [mA]	Real-EC (50 - 400)	30	30
Slice thickness [mm]	1.0	2.0	10.0
Reconstruction interval [mm]	1.0	1.0	10.0
Convolution kernel	FC01, FC10	FC01	FC01
The number of case	45	100	100

3.5 Identification of examined body part based on rules

The body parts have different features at multilayer structure and structure element. Firstly, the identification rules are constructed using learning data. Secondly, the body parts of input are identified based on the rules. For example, a rule for chest is as follows.

Rule 1: The multilayer structure is three layers.

Rule 2: The third layer is air.

Rule 3: A mass element is at the back of body.

The rule 1, 2 are based on the multilayer structure. And, the rule 3 is based on the structure element. All of rules are shown in Figure.8.

4. RESULTS AND DISCUSSIONS

We performed an experiment to evaluate the effectiveness of our method to 85 cases. The scan conditions are shown in Table.8. The 20 cases of torso examination are used for learning data, and 65 cases are used for test data. All of test data were identified as correct 5 parts. The results are shown in Figure.9. The parameters in each step are as follows. In the step.1, CT value threshold for bone is 100 [H.U.], and CT value threshold for air is -400 [H.U.]. In the step.2, the width of MIP is 40 [mm], the radius of Closing is 20 [mm], and the radius of small region is 20 [mm].

We measured the processing time of our method. The time is measured by a part image set. The time between step.1 and step.3 M_{Pre} is 2.5 [s]. The time on step.3 increases by the number of ellipsoids. And, the time M_i of an ellipsoid computation was influenced by area of the ellipsoid. In the case of small ellipsoid, the time M_i was 0.5 [s]. In the case of large ellipsoid, the time M_i was 1.0 [s]. Therefore, the processing time of all step M_{Total} are as follows. The N is the number of ellipsoids. For instances, the M_{Total} of the image shown third row in Figure.7 is 8.8 [s].

$$M_{Total} = M_{\Pr e} + \sum_{i=1}^{N} M_i \tag{3}$$

The results showed that our method can identify the examined body parts of CT images. In the borders between neighbor 2 body parts, the borders went a little up and down, because our method used MIP method and reduction of small regions. However, the importance of border determination is low.

The datasets for experiment vary in the scan conditions. Our method could identify the body parts without the influence of the variation in the scan conditions.

Our method is a preprocessing for CAD, and the processing time is important. Currently, we have not implemented any high speed algorithm and programming. This implementation is our future work.

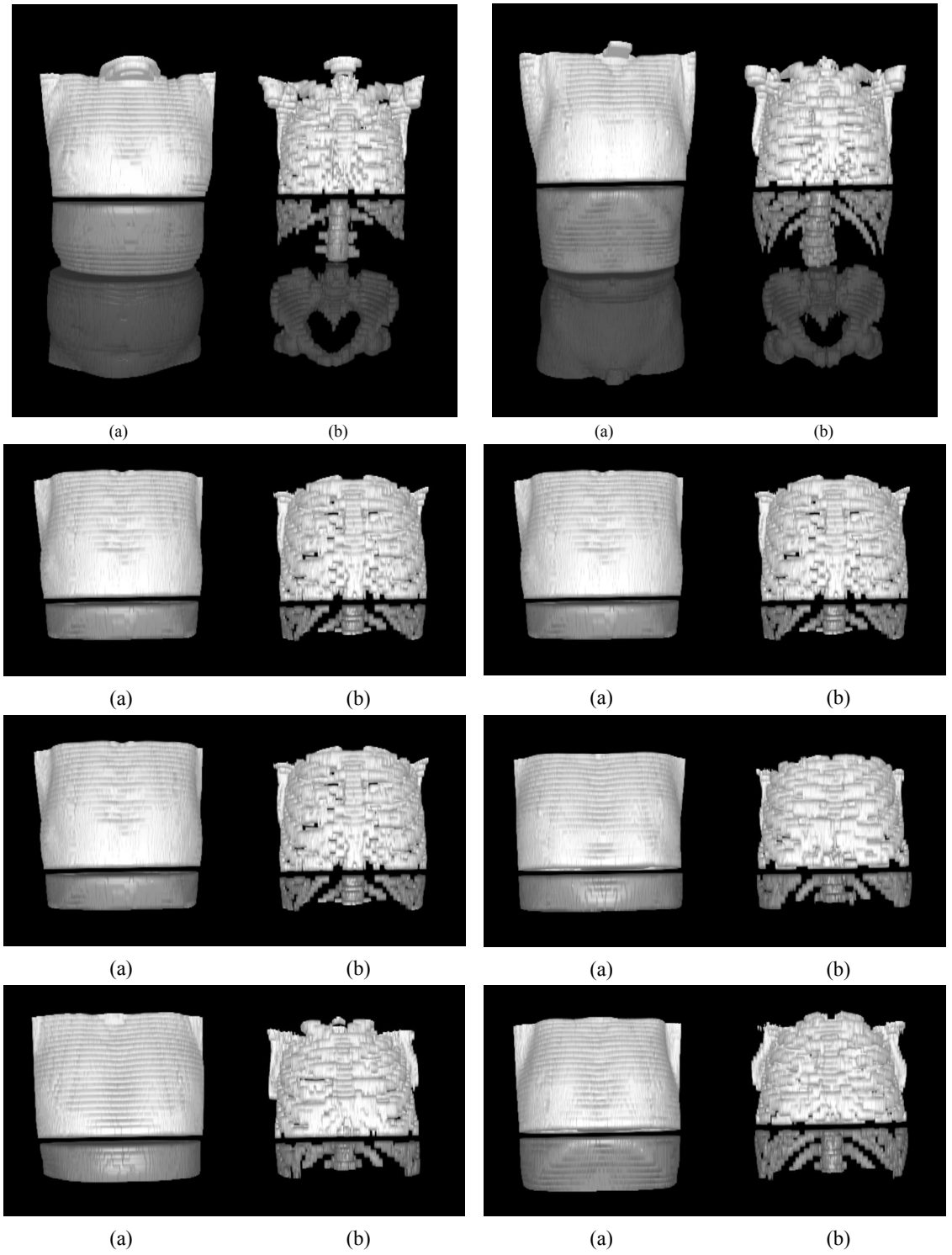

Figure.9. Results of the examined body part identification. The first row is torso. The second and third rows are chest with 2mm slice thickness. The fourth row is chest with 10mm slice thickness. (a) Labeled image of body tissue regions. (b) Labeled image of bone regions. The white, gray, and dark gray color mean chest, abdomen, and pelvis.

5. CONCLUSIONS

In this paper, we reported an automated distinction of DICOM images for lung cancer CAD system. The automated distinction of DICOM images is obviously necessary to the practical use of lung cancer CAD system in medical sites. Our method used both of DICOM textual meta information and image data. The examined body parts of CT images were identified using image data. The CT images were shown in bone, body tissue, and air. The features of the region were shown by multilayer structure and structure element. Our method is a preprocessing of CAD, and the processing time is important. In the future work, it is necessary to implement high speed methods, and to evaluate using large scale database.

REFERENCES

1. M. Kaneko, K. Eguchi, H. Ohmatsu, R. Kakinuma, T. Naruke, K. Suemasu, and N .Moriyama, "Peripheral Lung Cancer: Screening and Detection with Low-Dose Spiral CT versus Radiography," Radiology, vol.201, no.3, pp.798-802, 1996.
2. M. Kaneko, M. Kusumoto, T. Kobayashi, N. Moriyama, T. Naruke, H. Ohmatsu, R. Kakinuma, K. Eguchi, H. Nishiyama, E .Matsui, "Computed Tomography Screening for Lung Carcinoma in Japan," Cancer, vol.89, no.11, pp.2485-2488, 2000.
3. Masahiro Kaneko, et al, "Lung cancer screening with CT : Japanese experience ; the change and present conditions," Japanese Journal of Clinical Radiology, vol.49, No.3, pp.353-359, 2004.
4. Noboru Niki, "Development of Computer Aided Diagnosis for Lung Cancer CT Screening," IEICE Trans. Inf. & Syst. (Japanese Edition), vol.J91-D, No.7, pp.1715-1729, 2008.
5. H. Kobatake, "Future CAD in multi-dimensional medical images – Project on multi-organ, multi-disease CAD system," Comput. Med. Imaging Graph, vol.31, pp.258-266, 2007.
6. Y.Kawata, Y.Nakaya, N.Niki, H.Ohmatsu, K.Eguchi, M.Kaneko, N.Moriyama, "Measurement of three-dimensional point spread functions in multidetector-row CT," Proc. SPIE Medical Imaging, Vol.6913, pp.69131O-1-8, 2008.
7. National Electrical Manufacturers Association, "DICOM Standard," 2006.
8. Mark O. Guld, Michael Kohnen, Daniel Keysers, Henning Schubert, Berthold B. Wein, Jorg Bredno, and Thomas M. Lehmann, "Quality of DICOM header information for image categorization," Proc. of SPIE, vol.4685, pp.280-287, 2002.
9. Thomas M. Lehman, Mark O. Guld, Thomas Deselaers, Daniel Keysers, Henning Shubert, Klaus Spitzer, Hermann Ney, Berthold B. Wein, "Automatic categorization of medical images for content-based retrieval and data mining," Comput. Med. Imaging Graph, vol.29, pp.143-155, 2005.
10. Junich Hara, Hirokazu Kato, Seiji Inokuchi, "Description and Recognition of Animal Silhouette Image Using Ellipsoid-Expansion," IEICE Trans. Inf. & Syst. (Japanese Edition), vol.J74-D-II, no.3, pp.366-375, 1991.